Journal of Chromatography A, 1218 (2011) 2661–2667

Contents lists available at ScienceDirect

Journal of Chromatography A

journal homepage: www.elsevier.com/locate/chroma

Analyte migration in anisotropic nanostructured ultrathin-layer chromatography media

A.J. Oko [a], S.R. Jim [a], M.T. Taschuk [a], M.J. Brett [a,b,*]

[a] University of Alberta, Department of ECE, 2nd Floor ECERF, Edmonton, AB, Canada T6G 2V4
[b] NRC National Institute for Nanotechnology, 11421 Saskatchewan Drive, Edmonton, AB, Canada T6G 2M9

ARTICLE INFO

Article history:
Available online 13 December 2010

Keywords:
Thin-layer chromatography
Ultrathin-layer chromatography
Nanostructured thin film stationary phase
Glancing angle deposition
Anisotropic development

ABSTRACT

We investigate the performance of highly anisotropic nanostructured thin film ultrathin-layer chromatography (UTLC) media with porosity and architecture engineered using the glancing-angle deposition (GLAD) process. Our anisotropic structures resemble nanoblades, producing channel-like features that partially decouple analyte migration from development direction, offering new separation behaviours. Here we study GLAD-UTLC plate performance in terms of migration distance, plate number, retention factor and a figure of merit specific to GLAD-UTLC, track deviation angle. Migration distances increase with porosity by a factor of two for all feature orientations (up to a maximum of 22 mm) over the range of porosities considered in this study. Plate numbers approaching 1100 are observed for GLAD-UTLC plates when the nanoblade features are aligned with the development direction. We present a theoretical model describing mobile phase flow in anisotropic GLAD-UTLC media, and find good agreement with experimental results. Our plates provide channel features that reduce transverse spot broadening while providing the wide pores required for rapid migration and high separation performance. These improvements may enable a greater number of parallel separations on miniaturized GLAD-UTLC plate formats. Their small sizes should also make them compatible with the Office Chromatography concept in which office peripherals (inkjet printers and flatbed scanners) replace conventional TLC instruments. Equipped with a better understanding of the unique GLAD-UTLC elution behaviours, we expect to further improve performance in the future.

1. Introduction

Planar chromatography [1] is an effective method of performing rapid on-site chemical analyses in pharmaceutical testing [2,3], pesticide characterization [4], and food chemistry [5]. Thin-layer chromatography (TLC) is particularly appealing for its relative simplicity and its ability to analyze several samples in parallel. Minimal equipment is required since capillary forces drive the mobile phase across the porous TLC plate. As separated analytes remain on the plate, chromatograms may be extracted "off-line" and isolated species may be further characterized in complimentary methods such as mass spectrometry [6].

Since its inception, TLC has evolved into high-performance TLC (HPTLC) and ultrathin-layer chromatography (UTLC). The thinner layers and finer pore sizes of UTLC plates enable faster separations, shorter development distances, and higher sensitivities [7–9]. Continued UTLC stationary phase engineering efforts are motivated by the enhanced separation performance possible with controlled microstructure. Electrospinning offers an interesting approach to produce nanofibrous reversed-phase polymer [10] and glassy carbon [11] UTLC stationary phases. Other methods include physical vapour deposition of macroporous thin films.

Glancing-angle deposition (GLAD) is an established vacuum deposition technique for engineering porous columnar thin films in many useful materials and morphologies [12–14], and is a flexible platform for macroporous UTLC stationary phase study and design [15–17]. The first study of normal-phase silica GLAD-UTLC thin film media investigated elution dependence on porosity and microstructure [15]. Isotropic and anisotropic chromatographic media were comprised of hexagonal helices and chevrons, respectively. Rapid separations performed over short distances demonstrated that nanostructured GLAD-UTLC plates have a place within the new "Office Chromatography" concept [16]. Sample mixtures applied with an inkjet printer were separated on GLAD thin film UTLC plates in less than 60 s over ~10 mm and subsequently imaged with a flatbed scanner. Office peripheral performance exceeded that of dedicated TLC equipment, providing sufficient spotting and imaging precision to take advantage of miniaturised UTLC plates. The most recent investigation quantified GLAD-UTLC

* Corresponding author at: University of Alberta, Department of ECE, 2nd Floor ECERF, Edmonton, AB, Canada T6G 2V4. Tel.: +1 780 492 4438; fax: +1 780 492 2863.
E-mail address: mbrett@ualberta.ca (M.J. Brett).

0021-9673/$ – see front matter © 2010 Elsevier B.V. All rights reserved.
doi:10.1016/j.chroma.2010.12.021

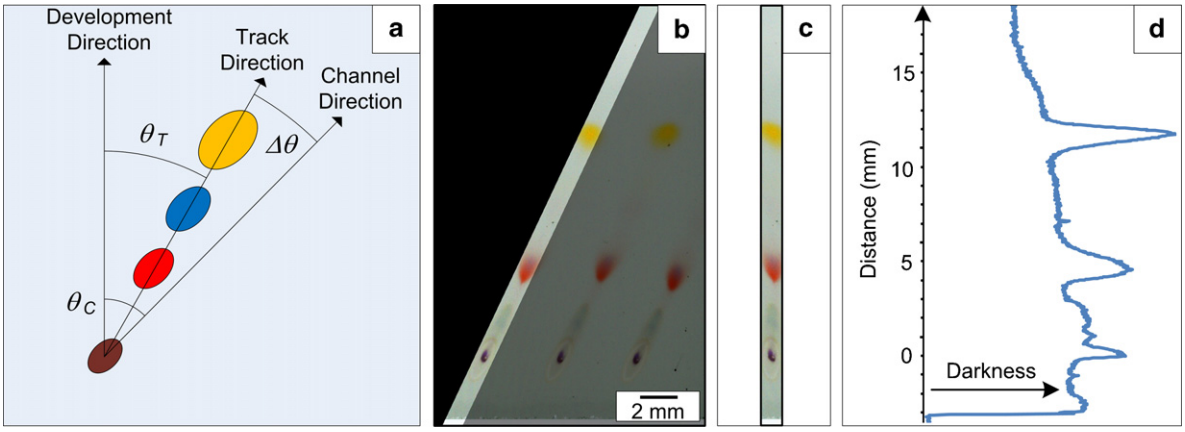

Fig. 1. (a) Schematic showing analyte separation and angle definitions. Track angle (θ_T) and channel angle (θ_C) are reported relative to development direction. (b) Image processing masks are created to isolate a separation track. One of the masks is partially transparent for clarity. (c) A representation of the cropped image with all unmasked pixel rows left-aligned. (d) Chromatogram displaying the average darkness (see Section 2.5) along each pixel row. Developed plate images enhanced for presentation.

plate performance with isotropic and anisotropic macropores using lipophilic dye separations [17]. Analyte migration and plate performance depended strongly on UTLC plate anisotropies, motivating a more thorough investigation.

In this paper, we report detailed investigations and modeling of anisotropic blade-like thin film chromatography media. UTLC plates of varied porosity and channel feature orientation were fabricated using GLAD and characterized using lipophilic dye separations. Migration distances up to 22 mm and plate numbers approaching 1100 were obtained. In addition, we present a theoretical model describing mobile phase flow in anisotropic media. The effect of film microstructure on UTLC figures of merit is discussed. Engineered GLAD-UTLC plates taking advantage of the unique elution behaviours studied here may improve performance over conventional planar chromatography methods.

2. Materials and methods

2.1. Glancing-angle deposition ultrathin-layer chromatography plate fabrication

The GLAD technique has been described previously [12–15,17], so only a brief review is given here. In GLAD, a substrate located within a high-vacuum physical vapour deposition system is maneuvered to achieve several thin film morphologies [12,13]. Manipulation of the film deposition angle (α) changes porosity [18] and surface area [19] while modulation of the azimuthal angle (φ) enables a variety of architectures including slanted posts, helices, vertical posts, chevrons, and anisotropic nanoblade structures. System base pressures were less than 100 μPa; deposition pressures varied between 460 μPa and 660 μPa. The deposition rate was held at approximately 8–10 Å s^{-1}, low enough to minimize φ-position errors. We deposited 5 μm thick (nominal) GLAD SiO_2 thin films on 1 in. square B270 glass substrates (Schott B270, S.I. Howard Glass, Worchester, MA, USA). Four deposition angles (α = 82.5°, 84.0°, 85.5°, and 87.0°) were chosen to produce films with different porosities; porosity increases with deposition angle [12,13,18]. A serial bideposition (SBD) film structure with a 24 nm period was grown [17,20]. The 24 nm period consists of four stages: 10 nm growth at φ = 0°, 2 nm uniform growth as φ changes from 0° to 180°, another 10 nm growth at φ = 180°, and finally 2 nm uniform growth as φ changes from 180° to 0°.

SBD structures are anisotropic in the substrate plane, resulting in well-defined channel-like features. Such channels may be oriented at an arbitrary angle with respect to the development direction (perpendicular to the top edge of the GLAD-UTLC plate). We define this angle as the "channel angle" (θ_C, shown in Fig. 1a). Nominal channel angles from 0° to 65° inclusive and 90° were obtained by orienting the edge of each glass substrate at the desired angle relative to the evaporant source direction during deposition. All samples were thoroughly cleaned with a dilute solution of Citrinox (Alconox, White Plains, NY, USA) and rinsed with deionized water prior to deposition. Films were also deposited on silicon wafers for scanning electron microscopy (SEM) characterization.

2.2. Analyte spotting

Test Dye Mixture III (CAMAG, Muttenz, Switzerland) was diluted in toluene (≥99.5%, Sigma–Aldrich Canada, Oakville, Ontario, Canada) to 50%. This diluted mixture contained 1.5 mg of Dimethyl Yellow, 0.25 mg of Oracet Red G, 1 mg of Sudan Blue II, 0.75 mg of Ariabel Red, 1 mg of Oracet Violet 2R, and 2 mg of Indophenol per mL of toluene (listed in descending hR_F). Spots were applied with a desktop dispensing robot (I&J 2200, I&J Fisnar, Wayne, NJ, USA). We manually dipped a 1/4 in., 32 gauge blunt end stainless steel tip needle (I&J Fisnar) into a small volume (~500 μL) of diluted test dye mixture before securing it onto the robot arm. Five spots were applied 4 mm apart along a line 3 mm from the bottom edge of the UTLC plate. At each spot the needle was rested against the plate for 1 s, allowing the diluted dye to wick into the film through capillary forces. This procedure resulted in estimated spot volumes between 2 nL and 10 nL.

2.3. Ultrathin-layer chromatography

We used a horizontal development chamber (Desaga H-Chamber, 50 mm × 50 mm, Sarstedt, Nümbrecht, Germany) similarly modified to that in [17]. The reservoir and conditioning trough were filled with the mobile phase (4:3 toluene:*n*-hexane; 95% *n*-hexane, Fisher Scientific, Ottawa, Ontario, Canada) at least 1 h prior to development to saturate the vapour phase. Spotted UTLC plates were loaded face-down into the chamber and aligned against the back glass spacer to control placement and angular orientation. Mobile phase in the reservoir continuously wicked up the porous glass frit and onto the face-down thin film stationary phase. Each plate was developed for 90 s and then removed from the chamber. An 1875 W hot air dryer was used to evaporate residual solvent by directing air opposite to the development direction at ~45° with respect to the plate normal.

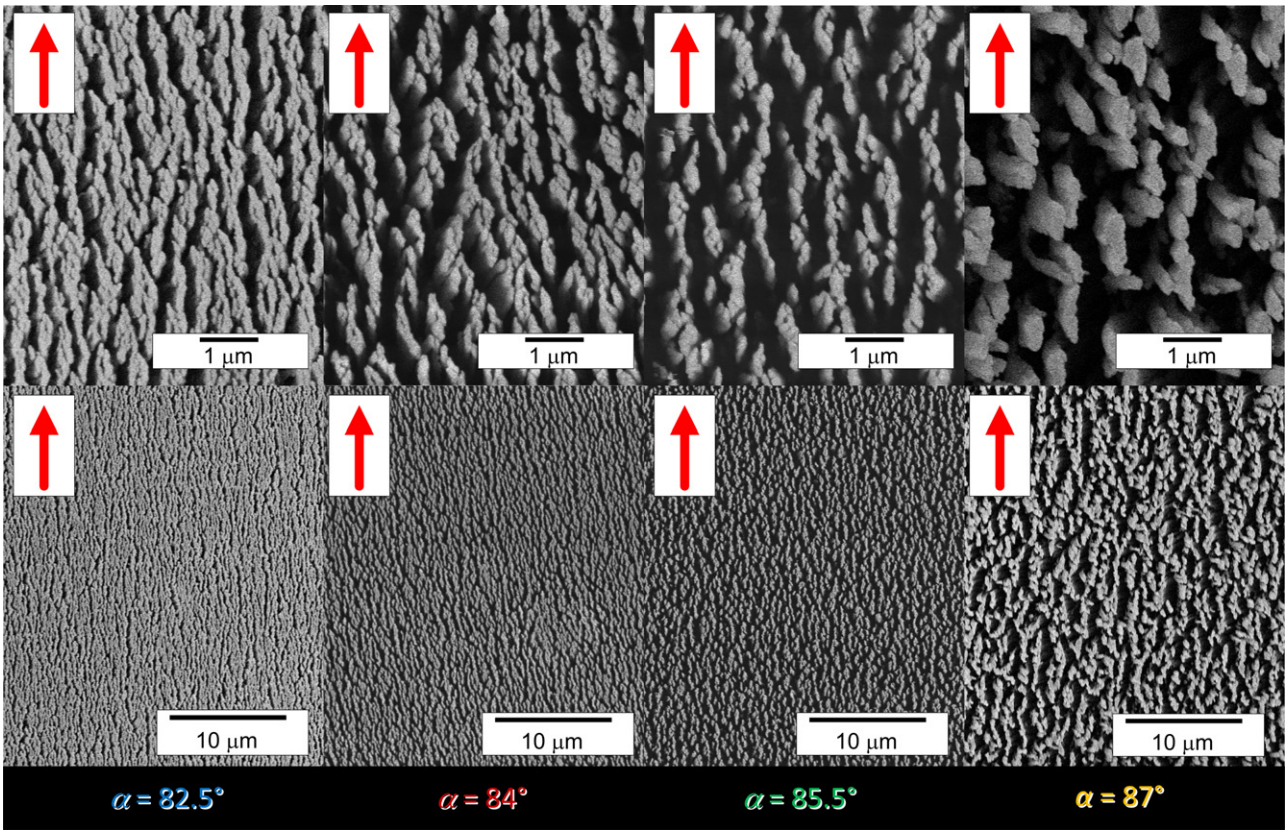

Fig. 2. High (top row) and low (bottom row) magnification scanning electron micrographs of 5 μm thick SiO_2 SBD films. Films deposited at higher deposition angle (α) are more porous. Arrows indicate the along channel direction (θ_C).

2.4. Anisotropy measurements

Samples were scanned before and after development using a flatbed film scanner (CanoScan 5600F, Canon, Mississauga, Ontario, Canada) in transmission mode. Photoshop (Photoshop CS3 Extended, version 10.0.1, Adobe Systems, San Jose, USA) was used to determine the channel and separation track angles from the high resolution (1200 dpi) scanned images. The channel orientation angle (θ_C) was measured from scans of undeveloped plates using an elliptical best fit to applied spots using ImageJ [21]. We used the Dimethyl Yellow spot to obtain accurate separation track measurements as this analyte travelled furthest. The angles reported here are an average and standard deviation for each sample. Some tracks at channel angles greater than 60° were distorted by our hot air drying technique; these tracks were excluded.

2.5. Chromatograms

Photoshop was also used to isolate each separation track. To clearly locate each track, scanned images were enhanced using a similar procedure to that described in [17]. Each track was masked to a constant pixel width along the development direction as seen in Fig. 1b. Track widths were chosen to match the analyte that broadened most during development, with typical values of 0.85 mm (40 pixels). The unenhanced, isolated tracks were saved as JPEG images, as in Fig. 1b, and imported into a custom script written for the MATLAB mathematical analysis software platform (MATLAB R2009a, version 7.8.0.347, MathWorks Inc., Natick, MA, USA) which calculates the average darkness value for each pixel row of the isolated track image [17]. Chromatograms were produced by plotting average darkness against development direction. Output from this analysis is shown in Fig. 1d.

3. Results and discussion

3.1. Plate nanostructure

Top down SEM images of our UTLC films are shown in Fig. 2 at different magnifications. The nanoblade SBD structure is clearly visible for all deposition angles. Image processing using ImageJ [21] was used to quantify some aspects of film morphology. Combined with a custom Python code [22], we were able to determine average edge-to-edge nanoblade spacing (channel width) and standard deviation of nanoblade orientation. The results are given in Table 1. The average channel width increases with deposition angle, reflecting the expected porosity dependence on deposition angle for GLAD films. However, spacing in the across-channel direction is poorly defined, and could not be quantified using the same analysis.

Also interesting is the increase in disorder with deposition angle. This value is reported as the standard deviation of the SBD nanoblade's orientation; a higher value indicates greater disorder. The post's preferential orientation decreases with increasing deposition angle. Increased variability in the channel walls may act to impede fluid flow, competing with the increased channel width.

Table 1
Morphological properties of SBD GLAD film posts. Channel width and the standard deviation of the nanoblade orientation (major axis of the SBD posts) increases with deposition angle.

Deposition angle (α) (degrees)	Average channel width (nm)	Nanoblade orientation standard deviation (degrees)
82.5	400 ± 20	15
84.0	670 ± 20	19
85.5	690 ± 20	21
87.0	840 ± 20	26

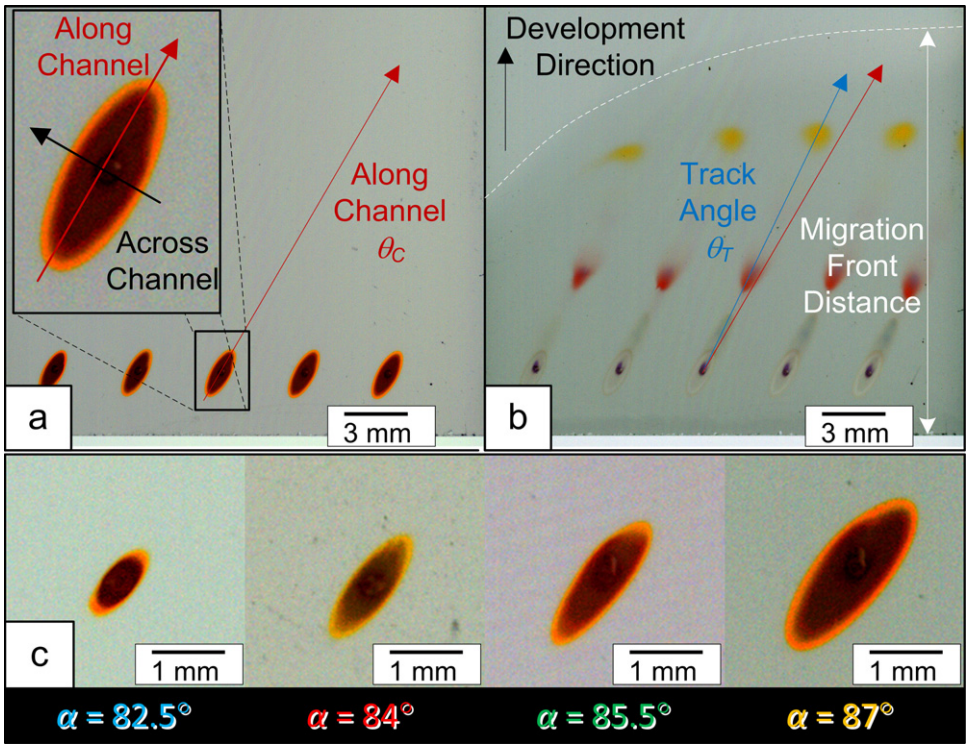

Fig. 3. (a) Applied spots broaden more in the along channel direction than in the across channel direction forming ellipsoids. (b) Fully developed plate with a small track angle deviation ($\Delta\theta$). Due to the films channel-like structure the migration front is curved. (c) Spot diffusion increases for larger α (greater porosity) and the spots' aspect ratios remain approximately constant. Plate images enhanced for presentation.

Fluid flow simulations may shed some light on the relative contribution of these effects.

3.2. Spot diffusion and plate development

Initial analyte spots were elliptical due to preferential diffusion in the along channel direction, as seen in Fig. 3. As expected, spot diffusion increases with increasing porosity (deposition angle) and is clearly visible in Fig. 3c. However, the aspect ratio (major to minor axis length; ~2–3) of the initial spots remained approximately constant with deposition angle. This suggests that the film's across-channel and along-channel diffusivities are changing at approximately the same rate, and thus the macropore anisotropy does not depend on deposition angle.

During chromatographic separation, the analytes migrated at a track angle that deviated a few degrees ($\Delta\theta$) from the channel angle (Fig. 3b). The separated analyte spots remained elliptical during development (Fig. 1a). The curved migration front seen on dried developed plates (Fig. 3b) is characteristic of differing channel and development directions and was consistent with that observed in [17]. The migration front is recorded in GLAD-UTLC plates through capillary-induced clumping of the film's nanostructure [23–25]. Although this front was visible in the GLAD thin films deposited at the higher angles ($\alpha = 85.5^\circ$ and $\alpha = 87.0^\circ$), it was difficult to accurately determine its location in those deposited at the lower angle ($\alpha = 82.5^\circ$ and $\alpha = 84^\circ$). This suggests that the effect of column clumping on the optical properties in wetted regions is suppressed in the denser films. When visible, the migration front distance was taken as the furthest distance the migration front travelled from the plate's bottom.

3.3. Dye separation analysis

To evaluate our nanostructured UTLC plate's utility in the anisotropic mode, we performed trial separations using the dye solution. Fig. 4 shows chromatograms and developed plates at all deposition angles. Porosity and channel widths increase with deposition angle, providing a more permeable stationary phase. This is reflected in the increased migration distances and improved separations observed at higher deposition angles.

The impact of developing on plates with different channel orientations is shown in Fig. 5 for a deposition angle of $\alpha = 87^\circ$. Separation track angle increases with channel angle, while migration distances decrease. The dye spots are still resolvable up to channel angles of $\theta_C \sim 60^\circ$; beyond this point all analytes remain too close to the original application spot to be resolved. Figs. 4 and 5 qualitatively demonstrate the range of separations made available by the GLAD-UTLC technique.

3.4. Quantification of separation performance

We have quantified our UTLC plate performance using migration distance, plate number and hR_F for Dimethyl Yellow (DY) and Ariabel Red (AR). The other dyes were of insufficient intensity and did not separate adequately to be quantitatively measured with our current chromatogram analysis methods. Analytes travelled further in the more porous (higher α) films. Fig. 6a shows migration distance increasing nearly by a factor of two for all channel angles as deposition angle increased from $\alpha = 82.5^\circ$ to 87.0°. The largest increase was from 10 mm ($\alpha = 82.5^\circ$) to 22 mm ($\alpha = 87.0^\circ$) in the along channel direction ($\theta_C = 0^\circ$). Plate number (N_i) was estimated from the darkness chromatograms using the following equation [26]:

$$N_i = 8 \ln 2 \left(\frac{Z_i}{W_i} \right)^2 \quad (1)$$

where Z_i and W_i are the peak migration distance and full width at half maximum of the ith analyte. Plate number for DY as a function of deposition angle and channel angle is shown in Fig. 6b. Conservative estimates of the plate number approach 150 and

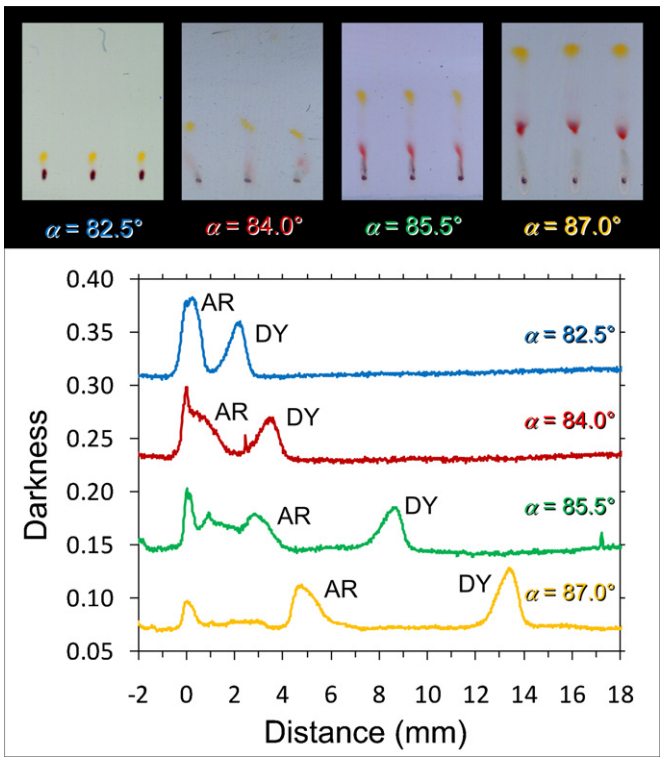

Fig. 4. Chromatograms for varying deposition angles in the along-channel direction ($\theta_C = 0^\circ$). Distances are referred to the initial spot position. The Dimethyl Yellow (DY) peak is clearly distinguishable for each deposition angle, while the Ariabel Red (AR) peak is only resolved at higher deposition angles. Developed plate images enhanced for presentation.

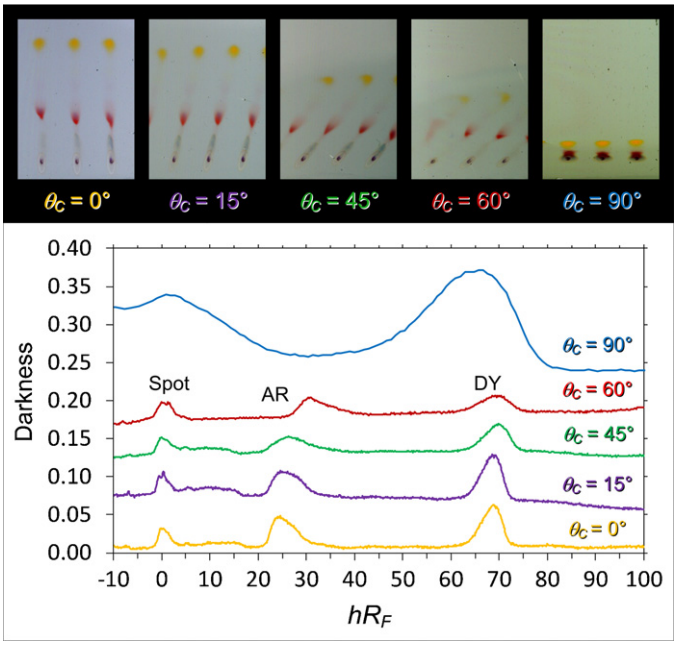

Fig. 5. Chromatograms from a $\alpha = 87^\circ$ SBD film at varying channel angles. The initial spot is located at $hR_F = 0$. Peak broadening is observed for increasing channel angles along with a slight shift in hR_f for both the Ariabel Red (AR) and Dimethyl Yellow (DY) peaks. The chromatograms are for each plate's center track. Developed plate images enhanced and peaks offset for presentation.

1100 for the Ariabel Red and Dimethyl Yellow, respectively. While these estimates do not compensate for the large initial applied spot sizes and their effects on reducing measured separation efficiencies, they enable characterization of some interesting trends. As expected, plate number improves with the increasing migration distances on plates with higher porosity. However, a decrease in plate number is observed with channel angle. Fig. 6 illustrates that the results reported here are consistent with our previously reported result for a deposition angle of $\alpha = 84^\circ$ [17]. The higher deposition angle ($\alpha = 87^\circ$) used here produces a factor of three improvement in plate number over those previously reported.

The DY and AR were easily distinguishable in the chromatograms shown in Figs. 4 and 5. Retention factors (hR_F) for these analytes are shown in Fig. 6c and d, respectively. The hR_F values for DY ranged between 20 and 70, whereas the AR varied by only 10 (from 20 to 30). Retention decreases with increasing deposition angle, most dramatically at a deposition angle of 82.5°. It was not possible to determine the AR hR_F for $\alpha = 84^\circ$ and $\alpha = 82.5^\circ$ since this analyte failed to separate from the initial spot over the 90 s development time.

3.5. Diffusivity ratio

We define θ_C and θ_T as the channel and track angles, respectively. By projecting the development direction onto the channel and separation track vectors, the track deviation angle ($\Delta\theta$) can be shown to be:

$$\Delta\theta = \theta_C - \theta_T = \arctan\left(\frac{1}{\sqrt{D}}\tan\theta_C\right) \quad (2)$$

where D is the diffusivity ratio between the along and across channel directions, respectively. A fit of this model to all $\Delta\theta$ data is given in Fig. 7, yielding a value for D of ~200. No dependence on deposition angle is observed, consistent with the spot diffusion observations reported in Section 3.2. While it is difficult to obtain precise data for the higher channel angles due to the short migration distances, the inset shows good agreement between the model and the track deviations observed at higher angles. Our previously reported $\Delta\theta$ values are consistent with those reported here [17]. For additional verification of the model, testing very porous films at $\theta_C > 60^\circ$ or increasing development time would be required.

3.6. Potential opportunities

The anisotropic GLAD-UTLC plates described above outperform those that we previously reported [17]. The increase in film deposition angle from $\alpha = 84.0^\circ$ to $\alpha = 87.0^\circ$ produces wider channels (from 400 nm to 840 nm) that produce faster migration velocities enabling higher separation performance. Although it is tempting to further increase the deposition angle, complications may arise as α approaches 90°. At extremely oblique deposition angles, the reduction in column density and surface area [19] will likely reduce analyte retention and overall separating power. Other potential disadvantages include further increase in column orientation disorder (as noted above) and impractically low deposition rates due to the extreme angle.

One promising result of the work reported here is the clear observation of DY quantities well below the limit of detection (LOD) reported previously [17]. In that work, we estimated our LOD for DY on GLAD-UTLC plates to be ~10 ng. The present paper demonstrates that DY masses as small as ~3 ng may be separated and detected on GLAD-UTLC media with similar equipment. The improved LOD is attributed to the use of smaller initial spots and suggests that sensitivity is currently limited by sample application methods. Further improvements in LOD and overall separation performance can be

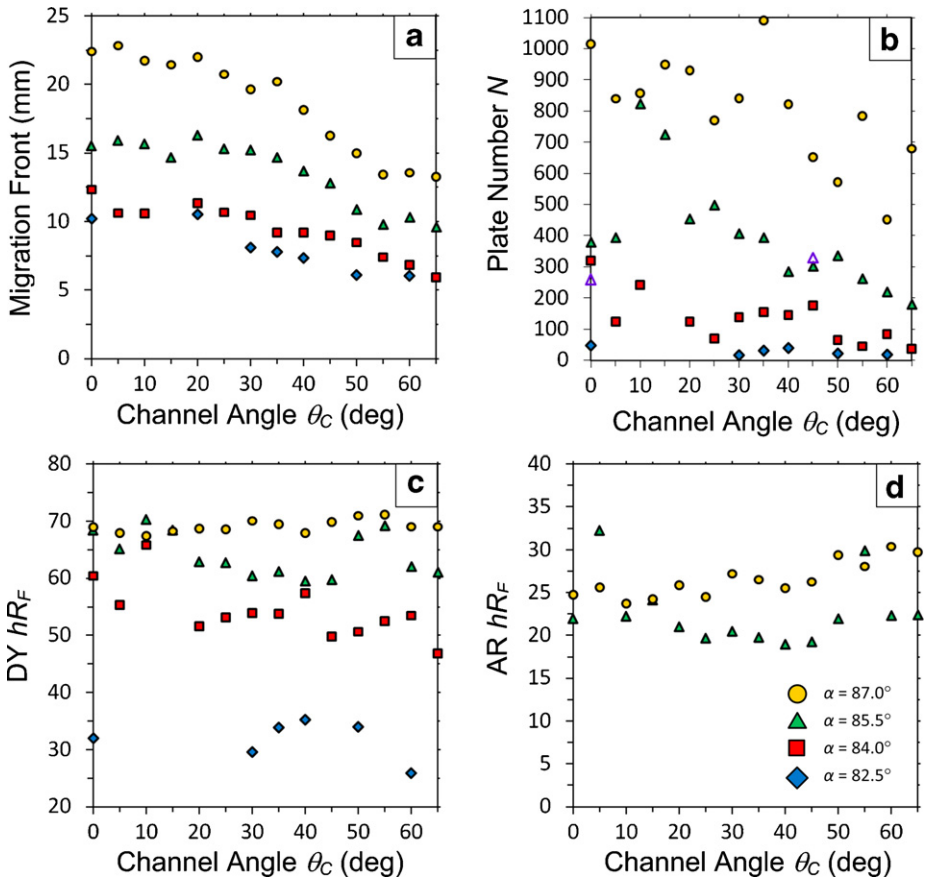

Fig. 6. (a) Migration front distances for 4 different deposition angles. (b) The large effect of deposition angle on plate number is observed for Dimethyl Yellow. The largest plate numbers obtained were for $\alpha = 87^\circ$ with a maximum of just under 1100. Open purple triangles located at channel angles of 0° and 45° correspond to the results obtained previously [17]. The Dimethyl Yellow (c) and Ariabel Red (d) retention factors were mostly independent of angle for a given film deposition angle. However, a noticeable change (up to 2×) in the retention factors can be seen for a 4.5° swing in α.

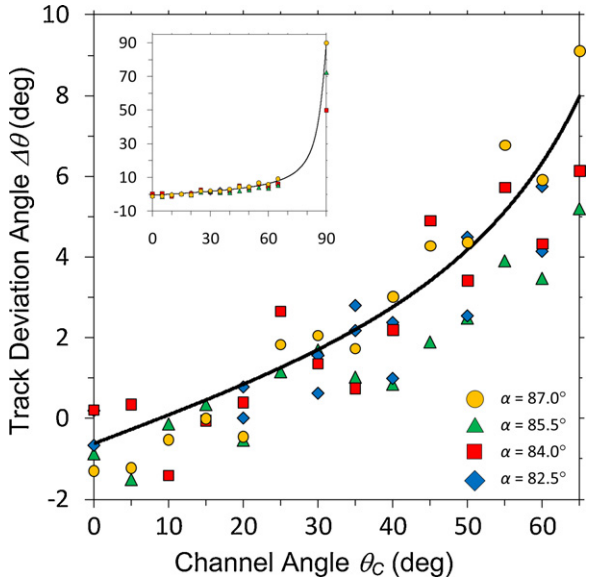

Fig. 7. Separation track deviation angle ($\Delta\theta$) as a function of channel angle (θ_C) for films grown at different deposition angles (α). $\Delta\theta$ is independent of deposition angle α. The solid line is a best fit of Eq. (2) to the entire data set. Inset shows good agreement between model and experimental data at very high channel angles.

expected if the analytes were applied with an inkjet printer. The smaller spots from inkjet application motivate continued work in coupling GLAD-UTLC media with the Office Chromatography concept [16].

Enhanced separation performance may also be achieved by adapting approaches developed for HPTLC over the past several decades. Attaching a highly porous pre-concentration zone [27] to a GLAD-UTLC plate may permit focusing of our broad spots into narrow bands prior to separation. Our media could also be amenable to the programmed multiple development technique [28]. The nanoblade features in the anisotropic media should permit spot compression through sequential elutions but suppress transverse broadening that would otherwise result from repeated exposures to the mobile phase. Forced-flow techniques such as over-pressured planar chromatography [29] and planar electrochromatography [30] could enable faster GLAD-UTLC separations and reduce diffusion broadening if the challenges posed by the thinner layers and narrower macropore sizes of our media can be overcome. Adapting circular and anticircular chromatography techniques established for isotropic HPTLC stationary phases [31,32] to our anisotropic GLAD-UTLC media may also produce useful new separation modes.

4. Conclusion

We investigated the channel-like features characteristic of anisotropic GLAD-UTLC media and their significant effects on chromatographic behaviour. We quantified GLAD-UTLC plate performance by characterizing migration distance, plate number, retention factor, and separation track deviation angle ($\Delta\theta$)—a figure of merit specific to anisotropic GLAD-UTLC. Migration distance and plate number increase with thin film deposition angle (film porosity) but decrease with channel angle (θ_C). We proposed a theoretical

model describing $\Delta\theta$ that relates analyte migration to anisotropic film microstructure. While not a focus of this study, we estimate Dimethyl Yellow LOD to be better than the ~10 ng value previously reported, likely due to the smaller initial analyte spots in this work. Application of sample spots with smaller volumes is expected to further improve LOD.

Channel features reduce transverse (across-channel) spot broadening during analyte application and elution while providing the wide (along-channel) pores required for rapid migration and high separation performance. As the channel structures reduce the interference between adjacent separation tracks, they enable the parallel analysis of several sample mixtures on the miniaturized GLAD-UTLC plate formats. Significant performance enhancements could be achieved by coupling these plates with the precise inkjet analyte application and high resolution chromatogram imaging offered by the Office Chromatography suite. An optimized GLAD-UTLC system that combines nanostructured chromatographic media with the advanced techniques originally developed for HPTLC and the benefits of office peripherals may become a part of the analytical chemist's toolset.

Acknowledgements

The authors are grateful for the financial support provided by the Natural Sciences and Engineering Research Council (NSERC) of Canada, Micralyne Inc. (Edmonton, Canada), and Alberta Innovates—Technology Futures. We also acknowledge the expert scanning electron microscopy work of G. Braybrook (University of Alberta Earth and Atmospheric Sciences SEM Lab).

References

[1] J. Sherma, Anal. Chem. 82 (2010) 4895.
[2] E. Reich, A. Schibli, High-Performance Thin-Layer Chromatography for the Analysis of Medicinal Plants, Thieme Medical Publishers, New York, 2007.
[3] J. Sherma, J. AOAC Int. 93 (2010) 754.
[4] J. Sherma, J. Environ. Sci. Health B 44 (2009) 193.
[5] G.E. Morlock, W. Schwack, J. Planar Chromatogr. Mod. TLC 20 (2007) 399.
[6] B. Fuchs, R. Süss, A. Nimptsch, J. Schiller, Chromatographia 69 (2009) S95.
[7] H.E. Hauck, O. Bund, W. Fischer, M. Schulz, J. Planar Chromatogr. Mod. TLC 14 (2001) 234.
[8] H.E. Hauck, M. Schulz, J. Chromatogr. Sci. 40 (2002) 550.
[9] H.E. Hauck, M. Schulz, Chromatographia 57 (2003) S313.
[10] J.E. Clark, S.V. Olesik, Anal. Chem. 81 (2009) 4121.
[11] J.E. Clark, S.V. Olesik, J. Chromatogr. A 1217 (2010) 4655.
[12] M.T. Taschuk, M.M. Hawkeye, M.J. Brett, in: P.M. Martin (Ed.), Handbook of Deposition Technologies for Films and Coatings: Science, Applications and Technology, 3rd ed., William Andrew (Elsevier), Oxford, 2010, p. 621.
[13] M.M. Hawkeye, M.J. Brett, J. Vac. Sci. Technol. A 25 (2007) 1317.
[14] K. Robbie, M. Brett, Method of depositing shadow sculpted thin films, U.S. Patent 5,866,204 (1999).
[15] L.W. Bezuidenhout, M.J. Brett, J. Chromatogr. A 1183 (2008) 179.
[16] G.E. Morlock, C. Oellig, L.W. Bezuidenhout, M.J. Brett, W. Schwack, Anal. Chem. 82 (2010) 2940.
[17] S.R. Jim, M.T. Taschuk, G.E. Morlock, L.W. Bezuidenhout, W. Schwack, M.J. Brett, Anal. Chem. 82 (2010) 5349.
[18] R.N. Tait, T. Smy, M.J. Brett, Thin Solid Films 226 (1993) 196.
[19] K.M. Krause, M.T. Taschuk, K.D. Harris, D.A. Rider, N.G. Wakefield, J.C. Sit, J.M. Buriak, M. Thommes, M.J. Brett, Langmuir 26 (2010) 4368.
[20] I. Hodgkinson, Q.H. Wu, Appl. Opt. 38 (1999) 3621.
[21] W.S. Rasband, ImageJ [Online], U.S. National Institutes of Health, Bethesda, MD, USA, 1997–2009, http://rsb.info.nih.gov/ij.
[22] Python Reference Manual [Online], http://docs.python.org/ref/ref.html.
[23] J.-G. Fan, D. Dyer, G. Zhang, Y.-P. Zhao, Nano Lett. 4 (2004) 2133.
[24] J.-G. Fan, Y.-P. Zhao, Appl. Phys. Lett. 90 (2007) 013102.
[25] J.-G. Fan, F.-X. Fu, A. Collins, Y.-P. Zhao, Nanotechnology 19 (2008) 045713.
[26] R.E. Kaiser, Trennzahlen [Online], Institute for Chromatography, Bad Duerkheim, Germany, 2010, http://www.internet-chromatography.com/html/trennzahlen.html.
[27] H. Halpaap, K.-F. Krebs, J. Chromatogr. 142 (1977) 823.
[28] T.H. Jupille, J.A. Perry, Science 194 (1976) 288.
[29] E. Tyihak, E. Mincsovics, H. Kalasz, J. Chromatogr. 174 (1979) 75.
[30] T.H. Dzido, P.W. Plocharz, P. Slazak, A. Halka, Anal. Bioanal. Chem. 391 (2008) 2111.
[31] R.E. Kaiser, J. High Res. Chromatogr. 1 (1978) 164.
[32] R.E. Kaiser, Micro Planar Chromatography [Online], Institute for Chromatography, Bad Duerkheim, Germany, 2009–2010, http://www.planar-chromatography-by-kaiser.com.